JOURNAL OF QUATERNARY SCIENCE (2022) 1–13 ISSN 0267-8179. DOI: 10.1002/jqs.3408

JQS Journal of Quaternary Science QRA Quaternary Research Association

Quaternary environmental changes in central Chukotka (NE Russia) inferred from the Lake El'gygytgyn pollen records

WENWEI ZHAO,[1]* ANDREI A. ANDREEV,[2,3,4] VOLKER WENNRICH,[4] QUAN LI[5,6] and MARTIN MELLES[4]
[1]School of Geographic Science, Nantong University, Nantong, 226007, China
[2]Alfred Wegener Institute Helmholtz Center for Polar and Marine Research, Research Unit Potsdam, Potsdam, 14473, Germany
[3]Kazan Federal University, Kazan, 420018, Russia
[4]Institute of Geology and Mineralogy, University of Cologne, Cologne, 50674, Germany
[5]Key Laboratory of Land Surface Pattern and Simulation, Institute of Geographic Sciences and Natural Resources Research, Chinese Academy of Sciences, Beijing, 100101, China
[6]University of the Chinese Academy of Sciences, Beijing, 100049, China

Received 14 April 2021; Revised 2 October 2021; Accepted 19 December 2021

ABSTRACT: The 3.6-Myr sedimentary record of Lake El'gygytgyn is crucial for understanding the response of the sensitive ecosystems in the Arctic to Quaternary climate variations at orbital timescales. In this study, we synthesize previously published pollen records and biome reconstructions and perform pollen diversity analysis of the deep-drilling core ICDP 5011-1 from Lake El'gygytgyn for periods during the Early Pleistocene (MIS 82 – MIS 79), Early–Middle Pleistocene (MIS 31 – MIS 18) and late Middle Pleistocene (MIS 7e – MIS 6f). The results indicate that the predominance of herb tundra in the regional vegetation was most characteristic during glacials/stadials. Interglacials, in contrast, can be distinguished by the expansion of shrub communities mainly composed of birch, alder and willow. The expansion of forest biomes in the region was influenced by peaks in obliquity values, which led to increases in daylight length, which was essential for plant growth in high latitudes. An apparent long-term decreasing trend in the tree and shrub population, accompanied by a reduction in floristic richness, was induced by stepwise cooling and drying since the Mid-Pleistocene Transition (MPT), which is linked to the modulation of extended global ice volume during the MPT via strong snow- and ice-albedo feedback effects. © 2022 John Wiley & Sons, Ltd.

KEYWORDS: glacial–interglacial cycles; ice–snow albedo feedback; Mid-Pleistocene transition; Milankovitch hypothesis; vegetation

Introduction

The oscillations between glacial and interglacial climates are the most fundamental characteristics of the Quaternary period (past 2.58 million years [Myr]; Shackleton and Opdyke, 1973; Shackleton *et al.*, 1990; Cohen and Gibbard, 2019). For more than a century, the cause of these climatic cycles has remained a research focus. According to the Milankovitch hypothesis (Milankovitch, 1941), the cyclical pattern of glacial–interglacial climates was primarily forced by Earth's orbital parameters: the precession (23-thousand years (kyr) and 19-kyr cycle), eccentricity (100-kyr cycle) and obliquity (41-kyr cycle). Investigations concerning the relationship between climate cycles and orbital parameters have been conducted on numerous geological archives of various depositional environments (e.g. Hays *et al.*, 1976). Much progress has been made based upon marine (e.g. Shackleton and Opdyke, 1976; Cronin *et al.*, 1994; Naish *et al.*, 1997, 1998) and ice-core records (e.g. Fischer *et al.*, 1999; Siegenthaler *et al.*, 2005). Long continental records, ideally spanning the whole Quaternary (e.g. Ding *et al.*, 2002; Prokopenko *et al.*, 2006; Sun *et al.*, 2019; Zhao *et al.*, 2020), in contrast, remain scarce. Consequently, our knowledge in particular about the long-term changes in the vegetation landscape is largely limited. The longest continuous vegetation records mainly come from the mid-latitudes, such as from the Zoige Basin on the eastern Tibetan Plateau [1.74 million years ago (Ma); Zhao *et al.*, 2020], Lake Ohrid in Macedonia (1.36 Ma; Wagner *et al.*, 2019) and Tenaghi Philippon in north-east Greece (1.35 Ma; Tzedakis *et al.*, 2006).

The Arctic is highly sensitive to climate variations and is thus a key region for understanding present and past continental climate changes. The longest continuous paleoclimate record as yet available from the Arctic originates from Lake El'gygytgyn (Fig. 1), a crater lake formed by a meteorite impact 3.58 ± 0.04 Ma in the Far East Russian Arctic (Layer, 2000). In 2009, an international deep-drilling campaign retrieved a composite core with 318 m of lacustrine sediments from Lake El'gygytgyn, which comprises the past 3.58 Myr (Melles *et al.*, 2011, 2012; Nowaczyk *et al.*, 2013). This record fills a large gap in the Quaternary environmental history in the high latitudes (e.g. Melles *et al.*, 2012; Brigham-Grette *et al.*, 2013; Francke *et al.*, 2013; Tarasov *et al.*, 2013; Wennrich *et al.*, 2013, 2016).

In the context of global climate change, it is important to investigate the long-term response of the modern and past ecosystems of the Arctic, such as tundra, forest tundra, shrub tundra and steppe tundra. As a powerful tool for reconstructing the paleovegetation, pollen analysis has been applied to the Lake El'gygytgyn sediments from composite core 5011-1. Andreev *et al.* (2014, 2016) presented pollen results of the lowermost 216 m of the sediment succession, documenting vegetation and climate changes during the Late Pliocene and Early Pleistocene (~3.58–2.15 Ma). For the same sediment core, Lozhkin and Anderson (2013) compared the pollen spectra of the Holocene Thermal Maximum and Marine

*Correspondence: Wenwei Zhao, as above.
E-mail: wenwei.zhao@foxmail.com

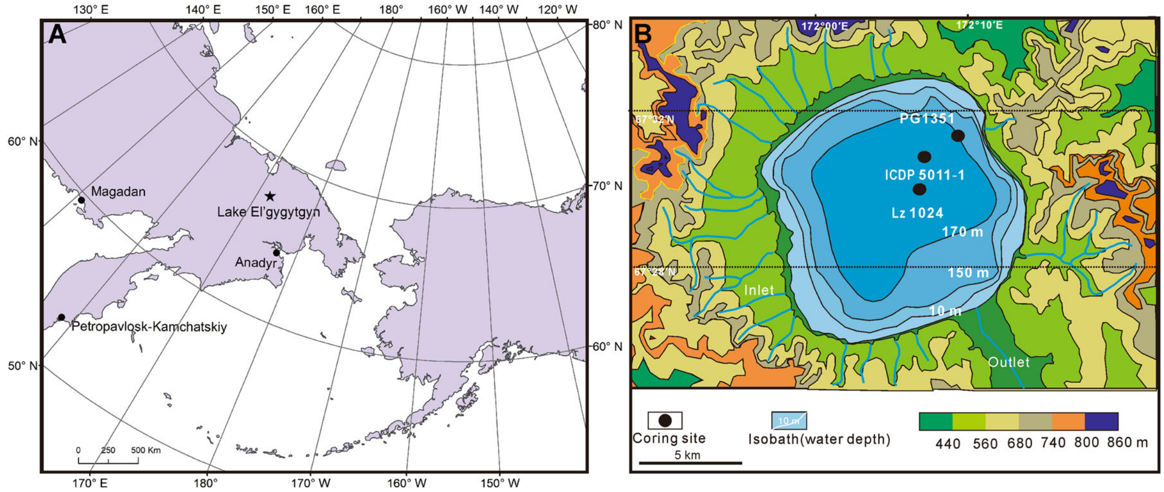

Figure 1. (A) Map of Beringia with the location of Lake El'gygytgyn marked by a star. (B) Bathymetric map of Lake El'gygytgyn and topography of its catchment after Swann *et al.* (2010), with the drilling sites ICDP 5011-1, PG1351 and Lz1024 indicated as black dots. [Color figure can be viewed at wileyonlinelibrary.com]

Isotope Stage (MIS) 5 with the 'superinterglacials' MIS 11 and MIS 31 (Melles *et al.*, 2012). More recently, Lozhkin *et al.* (2017) published a pollen record from core 5011-1 that encompasses a period of the mid-Pleistocene (MIS 19 – MIS 11; 374–790 ka). These pollen results confirmed the capacity of pollen spectra from central Chukotka, north-eastern Siberia, to document vegetation and climate changes at high sensitivity (Lozhkin *et al.*, 2006). In addition, 310 modern lacustrine samples were collected from north-eastern Siberia and Alaska and were analyzed to facilitate the interpretation of fossil pollen data (Anderson and Brubaker, 1993; Lozhkin *et al.*, 2001, 2002; Anderson *et al.*, 2002a,b).

By applying analysis of pollen diversity, combined with the previously published pollen-based biome reconstructions, we aim to provide deeper insights into the paleovegetation and its response to climate forcings in north-eastern Siberia during different stages of the Quaternary. For this, we synthesize our previous palynological investigation of the Lake El'gygytgyn sediment core 5011-1 for the intervals ~2150–2100 ka (MIS 82 – MIS 79; Zhao *et al.*, 2015), ~1091–715 ka (MIS 31 – MIS 18; Zhao *et al.*, 2018) and ~240.5–181.5 ka (MIS 7e – MIS 6f; Zhao *et al.*, 2019). The objectives are (i) to discuss the long-term trend in arctic vegetation and climate change from the Early Pleistocene, via the Early–Middle Pleistocene towards the late Middle Pleistocene, based on qualitative and quantitative pollen analysis; (ii) to discover the general characteristics and differences of vegetation succession during glacials and interglacials; (iii) to infer the response of arctic vegetation to changes in orbital forcings during different stages of the Quaternary; and (iv) to reveal possible mechanisms driving Quaternary vegetation and climatic variations in the high northern latitudes in comparison with vegetation records from the low and middle latitudes.

Study region

Lake El'gygytgyn is located ~100 km to the north of the Arctic Circle in north-eastern Russia (67°30'N, 172°05'E; Fig. 1A). It was formed by a meteorite impact ~3.58 Ma (Layer, 2000). The lake is 170 m deep and ~12 km in diameter (Melles *et al.*, 2012). The meteorite crater is a flat-bottomed circular basin ~18 km in diameter that is located on the south-eastern slope of the Akademik Obruchev Ridge in central Chukotka. The surrounding crater rim is elevated 100–130 m above the modern lake level (Fig. 1B). The lake has a surface area of 110 km^2 and a relatively small catchment of 293 km^2, with ~50 creeks discharging into the lake and the Enmyvaam River as the only outlet flowing south-eastward to the Bering Sea (Nolan and Brigham-Grette, 2006). The inlets deliver ~0.11 $km^3\ a^{-1}$ of water and ~350 $t\ a^{-1}$ of sediments into the lake, with spring and early summer being the main periods of inlet activity (Fedorov *et al.*, 2013). The discharge of the Enmyvaam River is limited to the summer months and is estimated to be ~0.05 $km^3\ a^{-1}$. The lake is covered by ice between mid-October and July (Nolan *et al.*, 2002).

The climate of northern Siberia is characterized by long cold winters and short hot summers (Shahgedanova *et al.*, 2002). Winters at Lake El'gygytgyn are marked by cold air masses brought by the strong Aleutian highs over the Beaufort and Chukchi Seas (Nolan and Brigham-Grette, 2006; Nolan, 2013). During summer, in contrast, warm Pacific air is transported into the area. Meteorological data between 1948 and 2002 for this region show a mean annual air temperature of −8.3 °C, ranging from −35 °C in winter to 8 °C in summer and an increasing trend in mean annual air temperature during the past decades (Kalnay *et al.*, 1996; Fig. 2). Mean annual precipitation in the El'gygytgyn crater is ~200 mm a^{-1}, with ~80 mm occurring during summer (from June to September) and ~110 mm as snowfall during the other seasons (Nolan and Brigham-Grette, 2006). Furthermore, strong winds are characteristic of the region, in particular during winter, when wind speed averages 17.8 m s^{-1}.

The regional vegetation in the Chukchi uplands is characterized by sparse tundra interspersed by a few low shrub species (Lozhkin *et al.*, 2006; Fig. 3). In the valleys, low shrubs, such as *Salix krylovii* and *S. alaxensis*, are found. *Betula exilis* is restricted to areas with better organic accumulation such as alpine valleys, terraces and saddles. In the southern Chukchi uplands, common shrubs are *Pinus pumila* and *Alnus fruticosa*. Open coniferous woodland appears ~150 km to the south and west of Lake El'gygytgyn. The northern taiga belt occurs at a distance of ~300 km, with *Larix gmelinii* being the most widespread deciduous tree.

In the El'gygytgyn Crater, riparian plants occur especially along the Enmyvaam outlet and large inlet creeks (Fig. 1B), consisting mainly of low shrubs of willow communities, such as *Salix tschuktschorum*, *S. saxatilis*, *Androsace ochotensis*, *Empetrum subholarcticum*, *Pleuropogon sabinii*, *Polemonium* spp.,

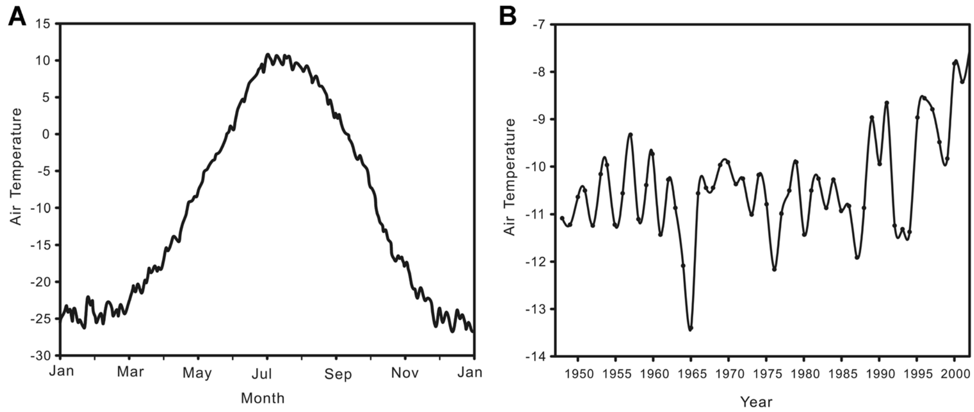

Figure 2. (A) Average daily air temperatures (°C) and (B) mean annual air temperatures (°C) in the Lake El'gygytgyn region for the period 1948–2002, derived from NCEP re-analysis data (after Nolan and Brigham-Grette, 2006).

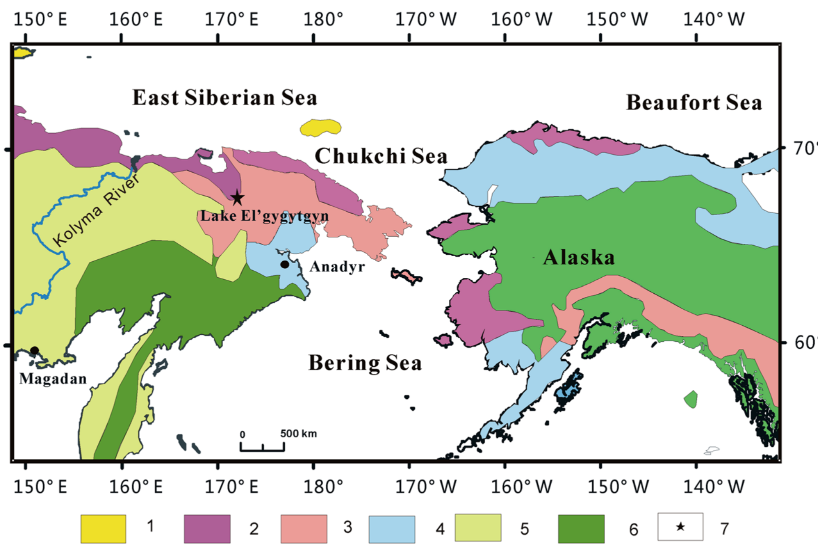

Figure 3. Vegetation map of Beringia, after Lozhkin *et al.* (2006): (1) polar desert with discontinuous herb-dominated vegetation, (2) wet arctic tundra dominated by *Eriophorum* spp. with some low-growth shrubs, (3) upland and mesic tundra, (4) moist tundra often with low- to mid-sized shrubs and Cyperaceae, (5) boreal forest dominated by *Larix gmelinii* and *Pinus pumila*, (6) high shrub tundra and (7) location of Lake El'gygytgyn. [Color figure can be viewed at wileyonlinelibrary.com]

Beckwithia chamissonis, *Saussurea tilesii* and *Chamerion latifolium* (Belikovich, 1994). The low-lying areas of the crater slopes and lake terraces are primarily covered by hummock tundra, with *Eriophorum vaginatum*, *E. callitrix*, *E. polystachion*, *Pedicularis pennellii*, *P. albolabiata*, *Carex rotundata*, *C. lugens*, *Salix fuscescens*, *S. reticulata*, *Senecio atropurpureus* and *Vaccinium uliginosum*. At higher elevations of the crater slopes, moss-lichen tundra occurs, being mainly composed of *Cassiope tetragona*, *Rhododendron parvifolium*, *Senecio resedifolius*, *Ermania parryoides*, *Silene stenophylla*, *Dryas octopetala*, *Potentilla elegans* and *Anderosace ochotensis*. The upper mountain plains are covered by polar desert, where *Salix phlebiphylla*, *Artemisia furcata* and *Saxifraga serpyllifolia* occur (Lozhkin *et al.*, 2001).

Materials and methods

Drilling campaign and sediment cores

The drilling operation on Lake El'gygytgyn was conducted by the US consortium DOSECC using a modified GLAD 800 drilling system (Russian GLAD 800) with funding mainly from the International Continental Scientific Drilling Program (ICDP), the USA, Germany, Russia and Austria (Melles *et al.*, 2011). Three parallel holes were drilled at ICDP Site 5011-1 in the central part of the lake (Fig. 1B). The drilling penetrated all sediments deposited since the formation of the lake and an additional ~200 m into the impact rocks beneath. Correlating a pilot core recovered in 2003 from the uppermost ~16 m (Lz1024) and the parallel cores from the ICDP campaign using magnetic susceptibility data, a core composite of 318 m length was obtained for the lacustrine sediment succession (Melles *et al.*, 2011). The core composite shows no signs of hiatuses due to glacial erosion or desiccation. The lacustrine sediments mainly consist of clastic particles and are highly variable in composition. Three major lithofacies were differentiated in the hemipelagic sediments and assigned to specific depositional conditions (for details see Melles *et al.*, 2012), along with mass movement deposits (Sauerbrey *et al.*, 2013) and fossil redox layers (Wennrich *et al.*, 2014).

Chronology

The El'gygytgyn impact was dated by $^{40}Ar/^{39}Ar$ on impact-melted rocks obtained from the crater rim to 3.58 ± 0.04 Ma (Layer, 2000). This age has been confirmed by paleomagnetic data measured on the impact breccia and bedrock material recovered by core 5011-1C (Maharaj *et al.*, 2013).

Age control on the lacustrine sediment record of core 5011-1 was obtained by an iterative tuning approach that was applied to tie points of three orders (Melles *et al.*, 2012; Nowaczyk *et al.*, 2013; Fig. 4). First-order tie points were provided by the age of the impact and by the geomagnetic polarity chrons (Gauss, Matuyama and Brunhes) as well as subchrons (Jaramillo, Olduvai, Réunion, Kaena and Mammoth), which were detected by paleomagnetic measurements on

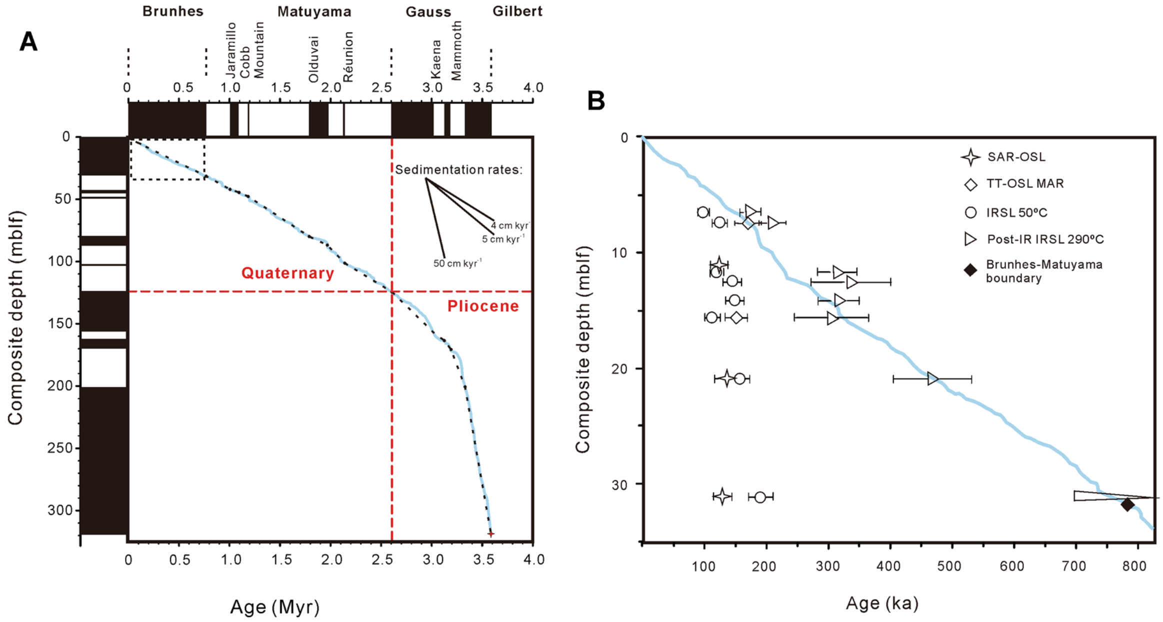

Figure 4. (A) Age/depth model for the lacustrine sediments in the core composite ICDP 5011-1 from Lake El'gygytgyn (after Melles *et al.*, 2012). The black dots indicate first-order tie points, the blue curve denotes second- and third-order tie points (for explanation see text), and the red cross marks the time of the meteorite impact at 3.58 ± 0.04 Ma. The black and white bars along the age and depth axes denote normal and reversed polarity, respectively. (B) Age/depth model for the uppermost 35 m of the core composite ICDP 5011-1 (blue curve) with the Brunhes/Matuyama polarity change (Haltia and Nowaczyk, 2014; black diamond) compared to independent luminescence ages (Zander and Hilgers, 2013; Wennrich *et al.*, 2016; open symbols). [Color figure can be viewed at wileyonlinelibrary.com]

U-channels and discrete samples. Second-order tie points were obtained by correlating the Si/Ti ratios and Ti (based on X-ray fluorescence scanning) and the biogenic silica (BSi) contents (based in Fourier transform infrared spectroscopy) with the global marine isotope stack LR04 (Lisiecki and Raymo, 2005). Third-order tie points were derived from the comparison of variations in the total organic carbon (TOC) contents and magnetic susceptibility (MS) with the cumulative 65°N summer insolation (Laskar *et al.*, 2004). The age/depth model derived for the uppermost 35 m was supported by luminescence ages determined on the fine-grained quartz and polymineral fractions (Zander and Hilgers, 2013). The dating protocols involved a multiple aliquot additive dose infrared stimulated luminescence (IRSL) protocol and a single aliquot regeneration dose (SAR)-IRSL protocol, which have been successfully applied to cores PG1351 (Forman *et al.*, 2006) and Lz1024 (Juschus *et al.*, 2009) of Lake El'gygytgyn sediments younger than 250 ka.

Pollen analysis, biome reconstruction and pollen diversity analysis

For the intervals from ~2.150 to 2.100 Ma (MIS 82 – MIS 79), ~1091 to 715 ka (MIS 31 – MIS 18) and ~240.5 to 181.5 ka (MIS 7e – MIS 6f) in core ICDP 5011-1, 371 samples were palynologically analyzed, with time resolutions of 1000, 2374 and 1067 years, respectively (Zhao *et al.*, 2015, 2018, 2019). For this, samples of ~1.5 g dry weight were subject to successive chemical treatments with HCl, KOH and HF, following acetolysis as described in Fægri and Iversen (1989). A tablet of *Lycopodium* marker spores was added to each sample to calculate total pollen and spore concentrations following Stockmarr (1971). If available, about 300 terrestrial pollen grains were counted in the samples using a light microscope at 400× magnification. Identification of pollen, spore and non-pollen-palynomorphs (NPPs) was in accordance with relevant palynomorph keys and atlases (Kupriyanova and Alyoshina, 1972; Bobrov *et al.*, 1983; Reille, 1992, 1995, 1998; van Geel, 2001).

As described in Zhao *et al.* (2015, 2018, 2019), pollen-based biome reconstruction (also known as biomization) was performed following the numerical method described by Prentice *et al.* (1996). The approach was first developed to produce a global vegetation map for the Last Glacial Maximum and the Holocene, which was a major task of the BIOME 6000 project (Prentice and Webb, 1998). For reconstructing past vegetation dynamics of a region, the biomization method introduces the calculation of biome affinity scores for each pollen sample using a standard equation. Fluctuations in the biome affinity scores can provide information regarding changes in the significance of a specific biome in the region. The method has been used in fossil pollen studies of different regions and has proved successful (e.g. Williams *et al.*, 2004; Rudaya *et al.*, 2009; Müller *et al.*, 2010; Chen and Litt, 2018). Based on the pollen data of 43 modern surface pollen samples collected in the Lake El'gygytgyn area (Matrosova, 2009), Tarasov *et al.* (2013) verified the reliability of the biomization approach and further applied biome reconstruction to previously published Lake El'gygytgyn core 5011-1 fossil pollen data in Lozhkin and Anderson (2013) and Andreev *et al.* (2014, 2016). The pollen-based index landscape openness has also been used for indicating the regional vegetation cover by calculating the difference between the maximal forest biome score (MSFB) and the maximal open biome score (MSOB).

In this study, we additionally performed pollen diversity analysis to reveal the changes in floristic diversity (Xiao *et al.*, 2008; Birks *et al.*, 2016; Felde *et al.*, 2016), following the method described by Li (2018). Pollen diversity indices, including pollen taxon richness (*S*), the sum of terrestrial pollen and spore types encountered in each sample (Gaston, 1996), the index of evenness (*E*), the variability in taxon abundances (Harper, 1999), the Shannon–Wiener index (*H*), and the estimates of both abundance and evenness of the pollen and spore taxa present (Shannon, 1948; Matthias *et al.*, 2015), were calculated employing the software PAST3 (Hammer *et al.*, 2001). Additionally, the index of palynological richness [$E(T_n)$, where n is the standard given number of pollen counts], allowing for standardization of differential palynomorph count-sizes, was applied using rarefaction techniques (Birks and Line, 1992). Rarefaction-based $E(T_n)$ has been used to reconstruct floristic diversity change over different time spans, such as the Holocene epoch (e.g. Birks and Line, 1992; Felde *et al.*, 2016; Liu *et al.*, 2021) and the glacial–interglacial cycles (e.g. Willis *et al.*, 2007; Whitney *et al.*, 2014). Here, the constant total sum of n was assigned as 300 grains, because the results of $E(T_{100})$ and $E(T_{200})$ are obviously biased by pollen count-sizes and $E(T_{300})$ is very similar to $E(T_{400})$ and $E(T_{500})$ (Supporting Information Fig. S1). Moreover, the sums of observed pollen and spores in this study are mostly 300 grains (ranging from 0 to 931 grains). The computations of $E(T_{300})$ and rarefaction analysis were undertaken by using the Incidence-based Coverage Estimator (ICE) of the software EstimateS 9.1 (Colwell, 2013).

Data synthesis and discussion

Arctic vegetation successions during the Quaternary glacial–interglacial cycles

Our previous palynological investigations of core ICDP 5011-1 cover the intervals from ~2150 to 2100 ka (including the Réunion Subchron polarity reversal event; Zhao *et al.*, 2015), ~1091 to 715 ka (representing the Mid-Pleistocene Transition, MPT; Zhao *et al.*, 2018) and ~240.5 to 181.5 ka (Penultimate Interglacial; Zhao *et al.*, 2019). In this study, all the pollen data are compiled and the pollen diversity indices of pollen taxon richness (*S*), evenness (*E*), Shannon-Wiener index (*H*) and palynological richness [$E(T_{300})$] are plotted along with a simplified pollen diagram (Fig. 5) to show the features of glacial and interglacial vegetation successions during the different Pleistocene intervals.

The result of rarefaction analysis shows that the index of pollen taxon richness (*S*) was biased by the differential count sizes among samples, while the values of palynological richness ($E(T_{300})$) remain relatively constant with increasing count size (Fig. 6), making it more robust as an indicator of floristic richness. To provide an overview of the long-term changes in Quaternary floristic richness, a boxplot of the index $E(T_{300})$ was made for the investigated periods of Early Pleistocene (MIS 82 – MIS 79), Early–Middle Pleistocene (MIS 31 – MIS 18) and late Middle Pleistocene (MIS 7e – MIS 6f) (Fig. 7A). In addition, separated boxplots were made for the interglacial and glacial samples during these periods (Fig. 7B,C), to distinguish the floristic richness during warm and cold stages, respectively.

The pollen assemblages indicate that tree and shrub populations, mainly composed of *Pinus*, *Picea*, *Larix*, *Alnus*, *Betula*, *Salix* and Ericales, were at maximum during the Early Pleistocene, followed by a gradual decline over the Early–Middle Pleistocene and relatively small values at the transition into the Late Pleistocene (Fig. 5). This is in line with

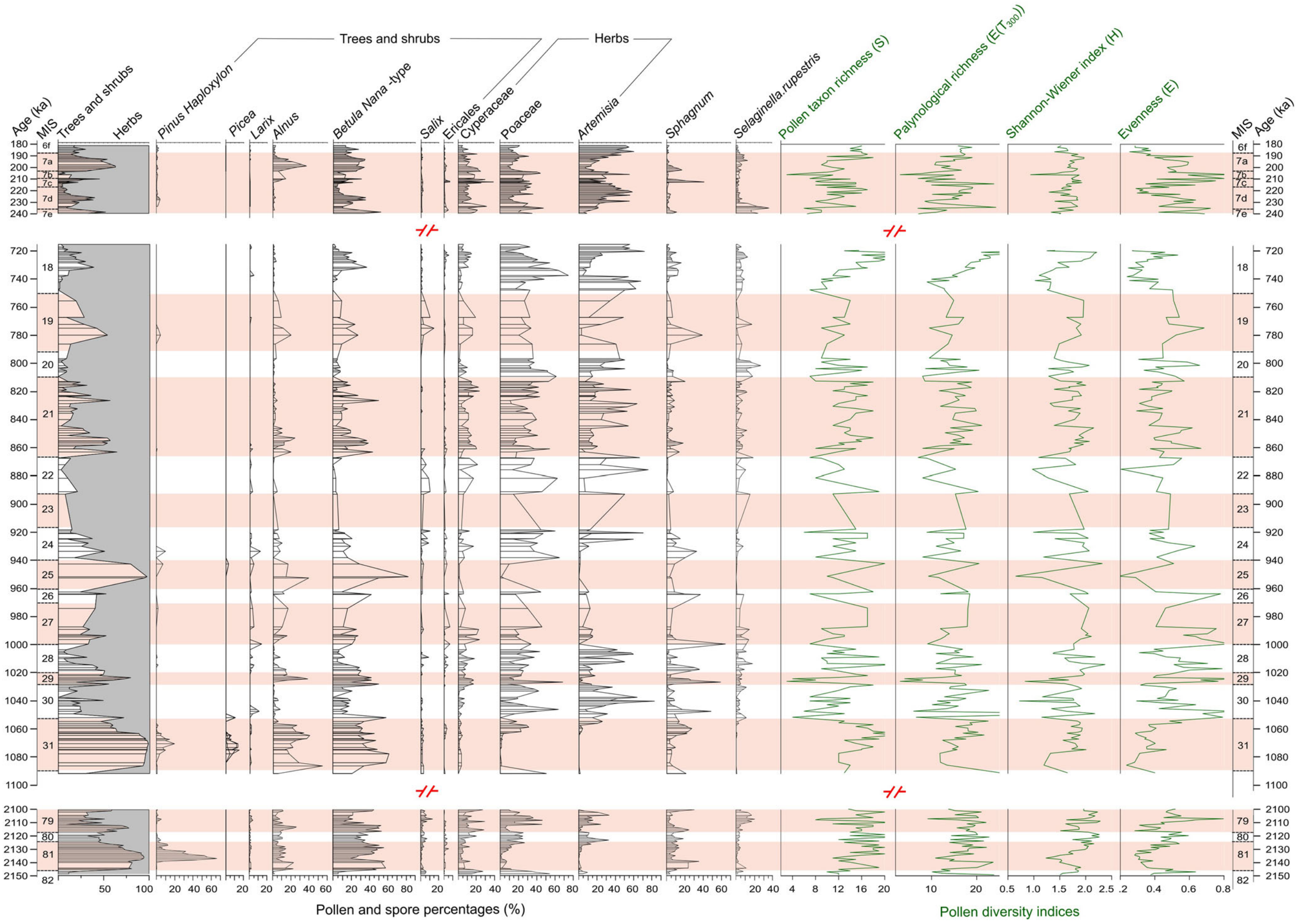

Figure 5. Summary diagram showing percentages of major pollen and spore taxa with pollen diversity indices of pollen taxon richness (*S*), palynological richness [$E(T_{300})$], Shannon-Wiener index (*H*) and evenness (*E*) of the Lake El'gygytgyn 5011-1 core sediments for the intervals 2150–2100 ka (MIS 82–79), 1091–715 ka (MIS 31–18) and 240.5–181.5 ka (MIS 7e–6f). The light red bands indicate interglacial periods. The breaks in the time scale indicate the time spans for which pollen data are not available in our study. [Color figure can be viewed at wileyonlinelibrary.com]

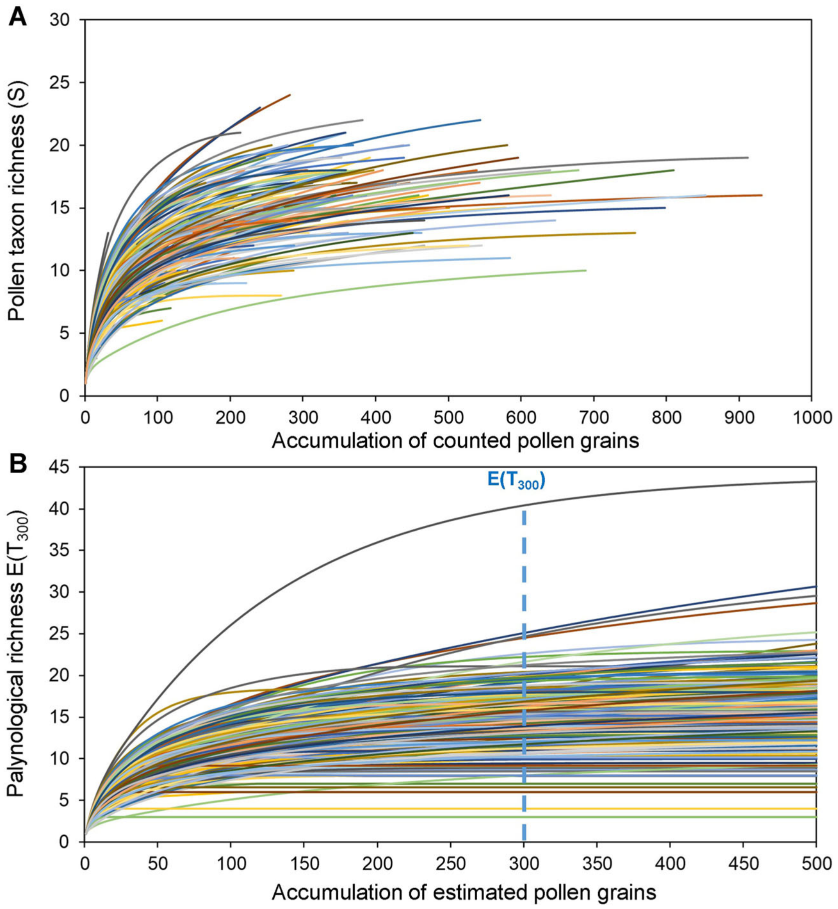

Figure 6. Rarefaction curves for (A) the index pollen taxon richness (*S*) and (B) the palynological richness [*E*(T_{300})], with the sum of pollen and spores encountered in each sample. [Color figure can be viewed at wileyonlinelibrary.com]

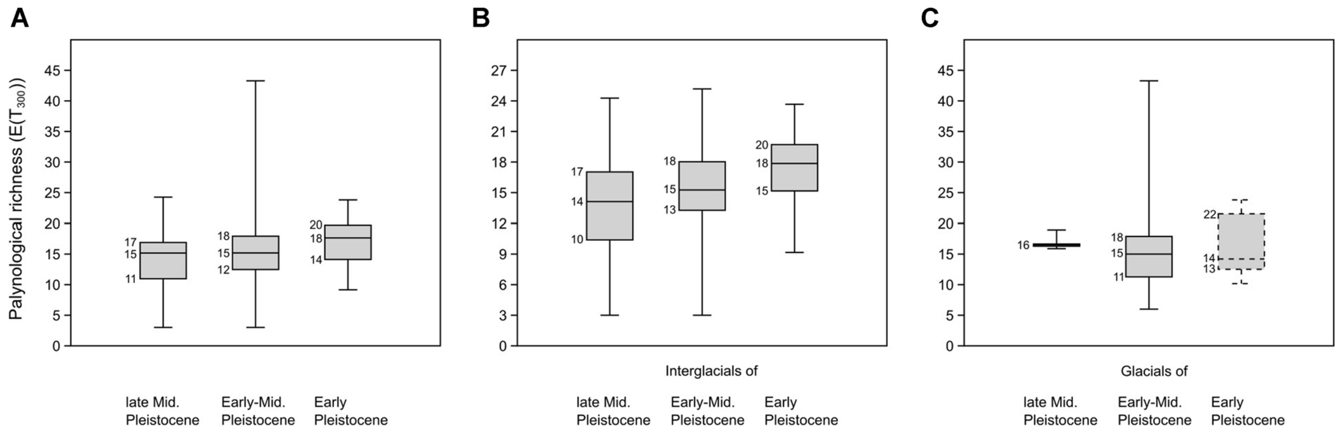

Figure 7. Boxplots of the pollen diversity index palynological richness (*E*(T_{300})) for (A) the investigated periods within late Middle Pleistocene (MIS 7e–6f), Early–Middle Pleistocene (MIS 31–18) and Early Pleistocene (MIS 82–79), (B) the interglacial and (C) the glacial samples in the respective periods. In C, note the glacial of Early Pleistocene is plotted with dashed lines as MIS 80 was the only complete glacial representing the Early Pleistocene in our study and it was possibly not a typical glacial because of the limited ice volume growth.

corresponding inverse changes in herbs, which took advantage of the more open landscape. From the pollen diversity analysis, the mean *E*(T_{300}) values for the Early Pleistocene, Early–Middle Pleistocene and late Middle Pleistocene decrease from 17.09, to 15.43 and to 14.13, and the corresponding mean *H* values from 1.86, to 1.70 and to 1.67, respectively. This reflects that the decrease in tree and shrub populations throughout the Quaternary was accompanied by a reduction in floristic richness.

Glacial vegetation succession

In general, the pollen assemblages during the glacials are characterized by (i) high contents of Poaceae and *Artemisia* pollen reflecting that tundra- and steppe-like communities dominated the local and regional vegetation; (ii) moderate percentages of *Salix* (regional shrubby taxa in the prostrate form), *Betula* and *Alnus*, along with small amounts of *Pinus* sect. *Haploxylon* (dwarf stone pine) pollen brought by wind from more distal areas; (iii) some *Larix* pollen from local trees growing at sheltered sites in the crater given the low production and poor preservation of *Larix* pollen (Andreev *et al.*, 2001; Kataoka *et al.*, 2003); and (iv) numerous spores of *Selaginella rupestris*, which grow in xeric and/or rocky habitats.

Despite these similarities, the glacial vegetation during different stages of the Quaternary also had individual characteristics. The Early Pleistocene (MIS 80) is notable by high contents of *Betula* and *Alnus* pollen (means of 30.1 and 7.4%, respectively) and low amounts of *Artemisia* and Poaceae pollen (means of 15.1 and 19.7%, respectively). The mid-Pleistocene glacial pollen spectra before the first large glaciation (MIS 24 – MIS 22) are characterized by relatively high Poaceae and *Artemisia* pollen percentages (means of 28.7 and 27.5%, respectively). Shortly after the first large glaciation, the glacial vegetation contained less shrubs, as indicated by very low shrub pollen contents (mean of <6.2%) and abundant *Artemisia* and Poaceae pollen (means of 38.5 and 35.9%, respectively). The Late Pleistocene (MIS 6 – MIS 2) pollen assemblages contain only very few pollen of shrubs (Lozhkin *et al.*, 2006).

These features indicate a general cooling trend throughout the glacials, with those during the Early Pleistocene being comparatively warm. Note, however, that MIS 80 as the only complete glacial period representing the Early Pleistocene in our study was possibly not a typical glacial because of the limited ice volume growth (Tzedakis *et al.*, 2017). Towards the Early–Middle Pleistocene, the xeric herb communities gradually increased at the expense of trees and shrubs, and the floristic diversity decreased (Fig. 7C). As a result, the vegetation landscape became more open and a long-term drying trend can be inferred for the regional climate. Nonetheless, among all the cold intervals (glacials/stadials), some were relatively wet, including MIS 80, MIS 30, MIS 28, MIS 26, MIS 24, MIS 7d and MIS 6f, because these periods were characterized by the presence of some *Pinus* sect. *Haploxylon* pollen, which suggests the presence of increased snow cover protecting this evergreen shrub from winter desiccation.

Interglacial vegetation succession

As compared to the glacials, interglacials can be distinguished by a predominance of shrubby components (*Betula–Alnus–Salix*) in the regional vegetation. The pollen spectra resemble the Holocene pollen assemblages detected in the pilot core PG1351 from Lake El'gygytgyn (Lozhkin *et al.*, 2006), and reflect similar warm climate conditions. Nevertheless, differences between the interglacials are also evident in terms of tree and shrub compositions.

First, the major pollen taxon of the MIS 81 optimum (mean of 44.8%; ranging from 28.4 to 65.8%), MIS 5 and the Holocene (Lozhkin and Anderson, 2013), *Pinus* sect. *Haploxylon*, had very low pollen percentages (<5%) during MIS 79, MIS 27, MIS 25 and MIS 21 possibly because of less winter snowfall. Second, the 'superinterglacials' MIS 31 and MIS 11 (Melles *et al.*, 2012) were marked by the establishment of dark green conifers (mainly *Picea* and *Pinus* sect. *Haploxylon*) and deciduous forests (mainly *Larix*) accompanied by tree and high-shrub *Betula* and *Alnus* both locally and regionally (Lozhkin and Anderson, 2013). Furthermore, interglacial MIS 25 is intriguing with regard to a more detailed vegetation reconstruction due to the exceptionally high percentages of *Betula* and *Alnus* pollen, indicating the presence of dense shrub stands in the region. Given the mild and short preceding glacial, MIS 25 was probably marked by more favorable environmental settings as compared to most other interglacials. However, herb pollen was almost absent, and other arboreal pollen was not found, contrasting with the pollen spectra of the 'superinterglacials' (e.g. MIS 31). Unfortunately, a higher resolution pollen analysis for MIS 25 is challenging, because most samples are of extremely low pollen concentration. In fact, information on the vegetation conditions for MIS 23 is missing, due to the near absence of pollen in the respective Lake El'gygytgyn sediments. MIS 23 as an interstadial (Tzedakis *et al.*, 2017) within the first large glaciation is interesting given the high TOC and BSi concentrations, as well as Si/Ti ratios of Lake El'gygytgyn sediments (Nowaczyk *et al.*, 2013). In this case, increasing the sample volume in future studies may yield enough pollen to reach an appropriate pollen sum.

In terms of vegetation successions, the interglacials preceding and following the first large glaciation show different patterns. Before MIS 24–22, the onset of most interglacials was characterized by a progressive increase in tree/shrub components. In contrast, most of the subsequent interglacials were initiated by a rapid expansion of trees and shrubs, followed by a gradual return to full glacial conditions. The cold deciduous forest (CLDE) biome of interglacials before MIS 24–22 was characterized by generally higher values and lower amplitudes of change than the cold steppe (STEP) biome, and vice versa for the interglacials after that (Fig. 8A). Although the number of interglacials and glacials included in this study is not enough for orbital cycle analysis, this phenomenon might be related to the symmetrical glacial–interglacial cycles of the '41-kyr world' and the more saw-toothed cycles of the '100-kyr world' (Maslin and Brierley, 2015). In response to the large-scale climate variations, a decreasing trend in floristic richness over the Quaternary is obvious also for the interglacials, as evidenced by the pollen diversity analysis (Fig. 7B).

Arctic biome variations during the Quaternary and the orbital forcings

The biome reconstruction provides a quantitative evaluation of vegetation changes that allows an explicit comparison with other paleoclimatic reconstructions (e.g. Tarasov *et al.*, 2013). Combining our biomization results for the periods 0–24 ka (MIS 1 – MIS 2), 90–140 ka (MIS 5), 380–430 ka (MIS 11) and 1091–1060 ka (MIS 31) with previous biome reconstructions from Lake El'gygytgyn core 5011-1 (Tarasov *et al.*, 2013), it becomes evident that north-eastern Siberia experienced prominent biome variations during the Quaternary (Fig. 8A). Five biomes existed in the region during the investigated periods, comprising tundra (TUND), cold steppe (STEP), cold deciduous forest (CLDE), taiga (TAIG) and cool conifer forest (COCO). The interglacials and glacials are characterized in particular by increases and decreases in CLDE biome affinity scores and simultaneous decreases and increases in STEP biome scores, respectively. The 'superinterglacials' MIS 31 and 11 differ from the other interglacials mainly by the high scores of two additional biomes, TAIG and COCO (Tarasov *et al.*, 2013).

The cyclical pattern of glacial–interglacial climate change was primarily forced by the variations in the Earth's orbital parameters: precession (23- and 19-kyr cycles), eccentricity (100-kyr cycle) and obliquity (41-kyr cycle; Hays *et al.*, 1976). According to Maslin and Ridgwell (2005), obliquity and precession are the dominant influences on glacial–interglacial cycles, whereas eccentricity 'paces' rather than 'drives' climatic change due to its very minor variations in the high latitudes. This is confirmed by the Lake El'gygytgyn biomization results, which show close associations with the changes in obliquity and precession (Fig. 8D).

During the early stage of most interglacials (i.e. MIS 81, 31, 29, 25, 21, 19, 11, 5 and 1), the onset of relatively high CLDE and/or TAIG and COCO biome scores corresponded with nearly simultaneous peaks of obliquity and precession (Fig. 8). The major control of obliquity and precession is expressed as a combined effect of daylight duration and summer insolation intensity, respectively, which are vital for vegetation successions in the high latitudes (Maslin and Ridgwell, 2005). Compared to lower latitudes, the high latitudes show a more

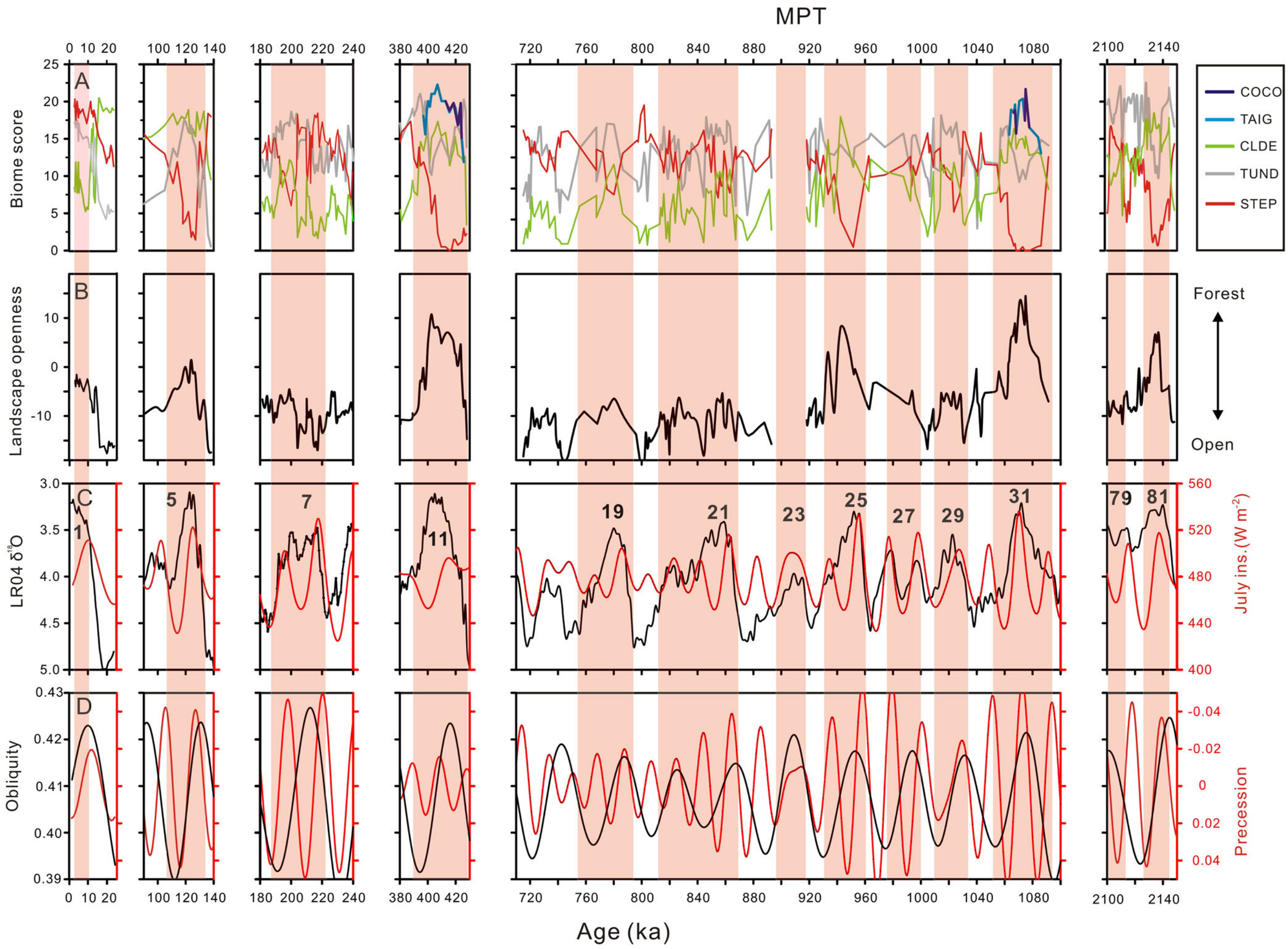

Figure 8. Summary diagrams showing: (A) biome reconstructions and (B) landscape openness calculated as the difference between MSFB and MSOB of ICDP 5011-1 core sediments for the intervals 2150–2100 ka (MIS 82–79, Zhao *et al.*, 2015), 1091–715 ka (MIS 31–18, Zhao *et al.*, 2018) and 240.5–181.5 ka (MIS 7e–6f, Zhao *et al.*, 2019), as well as for the intervals 0–24 ka (MIS 1–2), 90–140 ka (MIS 5), 380–430 ka (MIS 11) and 1091–1060 ka (MIS 31) according to Tarasov *et al.* (2013), (C) LR04 global marine stack (black line, Lisiecki and Raymo, 2005) and mean July insolation for 67.5°N (red line, Laskar *et al.*, 2004), and (D) precession (red line) and obliquity (black line), after Laskar *et al.* (2004). The light red bands indicate interglacial periods. MPT, Mid-Pleistocene Transition. [Color figure can be viewed at wileyonlinelibrary.com]

profound effect of obliquity on seasonal insolation (Berger and Loutre, 2004). For most interglacials, the particular importance of daylight length on Arctic plant growth highlights the significance of obliquity driving Arctic vegetation successions during the Quaternary, as evidenced by the in-phase changes between the CLDE biome scores and obliquity values in the Lake El'gygytgyn pollen record (Fig. 8). Changes in precession also played an important role. For instance, during MIS 79, 19 and 7, the increases in CLDE biome scores were minor, which might be explained by a weaker snowmelt during springs/summers and a relatively stabilized permafrost due to the offset in precession at 65°N.

Arctic vegetation and climate in response to internal forcings

In addition to the dominant influence of orbital forcings, internal forcings of the Earth system further modulated the regional vegetation and climate through snow- and ice-albedo feedbacks (Maslin and Ridgwell, 2005; Clark *et al.*, 2006), as inferred from the Lake El'gygytgyn pollen records. During the MPT, pronounced ice-sheet expansion led to significant sea-level lowering and exposure of continental shelves (Clark *et al.*, 2006). The consequently enhanced Siberian High and westerly jet may have caused long-term drying in the high latitudes following the first large glaciation (Clark *et al.*, 2006; Melles *et al.*, 2006). Moreover, the climate cooling might have been intensified by the concomitant uplift of the north-eastern Tibetan Plateau after ~0.9–0.8 Ma (Ruddiman and Kutzbach, 1989; Li, 1995; Fang *et al.*, 2005, 2007). The prominent cooling probably resulted in a subdued snowmelt and an expanded ice sheet that aggravated the Earth-albedo feedback (Calov *et al.*, 2005). As a consequence, deep permafrost was widely distributed in the Arctic and the growth of trees and shrubs was hampered.

The duration and state of each warm stage (interglacial/interstadial) differ between one another, as reflected by the Lake El'gygytgyn pollen spectra and biome reconstructions. Apart from the differential orbital configurations, Herzschuh *et al.* (2016) suggest that the climate conditions of preceding glacial/stadials had strong imprints on the subsequent warm intervals in the high altitudes at the Pliocene–Pleistocene transition. This phenomenon is also indicated by the pollen records presented here, in particular for the warm periods of MIS 21, 19 and 7 (Figs. 5 and 8).

As the most prominent example, MIS 7 involves three warm intervals (MIS 7e, 7c and 7a) and two cold intervals (MIS 7d and 7b). The climatic optimum occurred during substage MIS 7a (~10-kyr duration), as identified by maximum arboreal pollen contents and highest CLDE biome affinity scores (Figs. 5 and 8).

In addition to the persistently high precession-induced summer insolation, MIS 7a was preceded by the mild and short-lived MIS 7b stadial. As a result, the arboreal refugia were probably close to the Lake El'gygytgyn area and the permafrost was only moderately distributed.

In contrast, MIS 7e and 7c were short (~4-kyr duration) and characterized by much fewer trees and shrubs under relatively disadvantageous orbital settings (Figs. 5 and 8). Both intervals were preceded by a long and cold glacial/stadial (MIS 8 and MIS 7d, respectively). In particular, the MIS 7d stadial was marked by a large glaciation (Tzedakis *et al*., 2003), which was triggered by coevally low values of obliquity and precession-induced summer insolation. The significantly reduced summer temperatures probably resulted in strong snow- and ice-albedo feedback. Consequently, the permafrost may have been extensive and stabilized, thus preventing trees and shrubs from spreading.

Comparisons with the MPT in mid- and low-latitude climate records

The MPT is a prominent climate event in the Quaternary. The marine oxygen isotope records show that the MPT began 1250 ka and ended at 700 ka, reflected by a gradual increase in average global ice volume (Clark *et al*., 2006). This is in line with the MPT at Lake El'gygytgyn, indicated for instance by the sedimentary grain-size record of the core composite ICDP 5011-1 (1250–670 ka, Francke *et al*., 2013). Investigating the response of vegetation to the MPT in different latitudes can deepen our understanding into feedback mechanisms in each of these climate systems. Although continuous vegetation records encompassing the MPT are rare, vegetation changes throughout the MPT in the mid- and low latitudes are particularly well reflected in the Tenaghi Philippon pollen data from the eastern Mediterranean, Greece (Tzedakis *et al*., 2006), and alkenone data from the Angola Basin, eastern tropical Atlantic (Schefuß *et al*., 2003), respectively (Fig. 9B,C).

In the early stage of the MPT, the onset of the MIS 31 'superinterglacial' in the high latitudes may have been triggered by synchronous peaks of precession and obliquity that led to high summer insolation intensity and long daylight (1062–1078 ka, Melles *et al*., 2012). This coincides with a strikingly limited global ice volume, as reflected by the lowest oxygen isotope values in the benthic LR04 stack (Lisiecki and Raymo, 2005; Fig. 9D). With analogous orbital configuration, MIS 25 in both high and mid-latitudes was characterized by a regionally forested landscape (Fig. 9A,B). These two interglacials were separated by the weak MIS 27 and 29 interglacials as a result of relatively low precession and obliquity values. In the low latitudes, during the early stage of the MPT, the gradual cooling of the tropical Atlantic (Schefuβ *et al*., 2004) did not follow the saw-tooth-like pattern as observed in the LR04 benthic $\delta^{18}O$ record. Instead, glacials appeared relatively rapidly and are reflected by sharp drops in sea surface temperatures (SSTs) (Fig. 9D). According to Schefuβ *et al*. (2004), tropical SST declines resulted in large-scale aridification and favored the establishment and expansion of C_4 grassland in tropical West Africa (Fig. 9C). Similarly, pollen records in the tropical high Andes, Columbia, reveal that severe drought caused the drastic contraction of montane forest (Torres *et al*., 2013).

The middle stage of the MPT (MIS 24 – MIS 22) is a remarkable interval characterized by the first large glaciation, extreme SST cooling and a reduction in thermohaline circulation (Schmieder *et al*., 2000; Clark *et al*., 2006). For example, the sedimentary sequences along the Japan Sea coast indicate that eustatic sea level was 20–30 m lower during MIS 22 relative to MIS 28 (Kitamura and Kawagoe, 2006), pointing

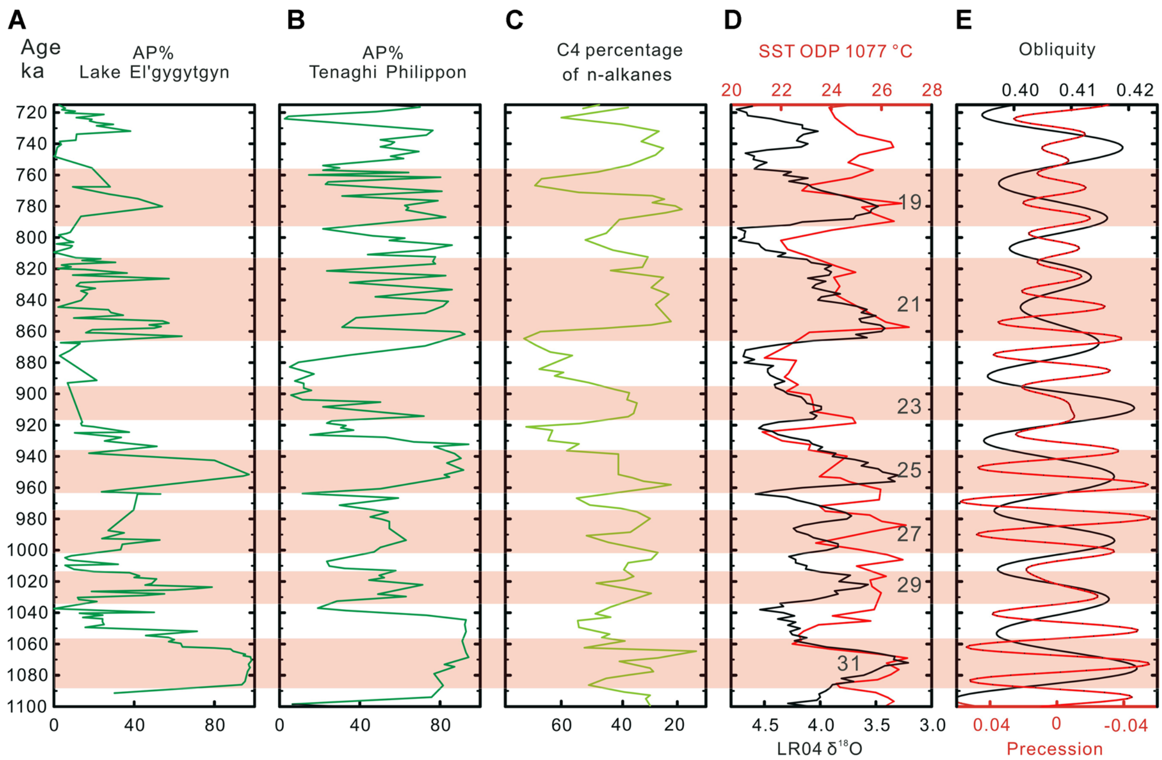

Figure 9. Correlation of paleorecords in different latitudes for the Mid-Pleistocene Transition (MPT). (A) Tree and shrub pollen (AP %) in core ICDP 5011-1 from Lake El'gygytgyn, Russian Arctic. (B) AP percentages in the record from Tenaghi Philippon, Greece (Tzedakis *et al*., 2006). (C) C_4 plant fraction of the plant wax n-alkanes using $\delta^{13}C$ values of the n-C31 alkane, in sediment core ODP 1077 from tropical West Africa (Schefuß *et al*., 2003). (D) Alkenone-derived SST (°C) record at ODP Site 1077, tropical Atlantic Ocean (red line; Schefuß *et al*., 2004), and LR04 global marine isotope stack marked with numbers of marine isotope stages (black line; Lisiecki and Raymo, 2005). (E) Global precession (red line) and obliquity curves (black line), after Laskar *et al*. (2004). [Color figure can be viewed at wileyonlinelibrary.com]

to the increase in ice volume and a substantial cooling event at ca. 900 ka (Clark *et al.*, 2006). Unfortunately, extremely low pollen concentrations in the Lake El'gygytgyn MIS 23 sediments, probably a result of sparse vegetation cover, make it impossible to analyze the mechanisms behind the vegetation change in the high northern latitudes during this period. In the eastern Mediterranean, trees and shrubs during MIS 23 were much less floristically diverse compared to typical interglacials, while herbaceous taxa remained important components in the vegetation (Tzedakis *et al.*, 2006). At the same time, tropical West African C_4 plants significantly expanded because of a cooling tropical Atlantic and reduced thermohaline circulation (Schefuß *et al.*, 2003). These phenomena might be closely linked to the intermediate caloric summer insolation peak of MIS 23 as well as the short elapsed time since MIS 25 (Tzedakis *et al.*, 2017). As a result, the insufficient effective energy of MIS 23 failed to initiate deglaciation, which led to the long glaciation from MIS 24 to MIS 22.

Following the interval of MIS 24–22, the late stage of the MPT was characterized by limited summer insolation intensity and daylight duration that may have prevented snow from melting and led to an extended global ice volume (Lisiecki and Raymo, 2005; Fig. 9D) and lower deep-water temperatures (Clark *et al.*, 2006). This in turn may have caused strong Earth-albedo feedback effects that aggravated glacial conditions in accordance with climate modeling studies (Calov *et al.*, 2005; Liu *et al.*, 2020). As a result of the prominent cooling trend, even though with an orbital configuration similar to that during MIS 29 – MIS 27, a relatively more open landscape persisted in the high northern latitudes in the late stage of the MPT. This cooling trend is also closely linked to the long-term forest contraction in the eastern Mediterranean region (Tzedakis *et al.*, 2006; Fig. 9B). By contrast, in tropical West Africa, C_4 plant expansion was suppressed by the prominently strengthened thermohaline circulation and long-term warming of the tropical Atlantic Ocean that was probably generated by extremely northward displaced Southern Ocean Fronts (Schefuß *et al.*, 2004; Fig. 9C,D). Nevertheless, the SST-induced vegetation variations in the low latitudes are of a higher amplitude and are in phase with glacial–interglacial cycles since the middle stage of the MPT.

The above observations show that vegetation in the high, mid- and low latitudes demonstrates different reactions to the MPT in different climate systems. It appears that low-latitude vegetation dynamics are more closely linked to tropical SSTs changes and show a weaker connection with glacial–interglacial cycles compared with that of the high and mid-latitudes, especially during the early stage of the MPT. Nonetheless, an increasingly important impact of the mean state and frequency of ice volume variations on tropical vegetation and climate since the middle MPT is evident.

Conclusions

Synthesizing previously published results from palynological analysis and biome reconstruction for the periods MIS 82 – MIS 79, MIS 31 – MIS 18, MIS 11, MIS 7e – MIS 6f, MIS 5 and MIS 1 – MIS 2 from drill core ICDP 5011-1 from Lake El'gygytgyn, and further analyzing the pollen diversity, the following conclusions can be drawn.

1. The vegetation of cold intervals (glacials/stadials) at Lake El'gygytgyn was dominated by herb tundra. Some of the cold intervals were characterized by increased snow fall, supporting the survival of some stone pines by increased snow cover. In contrast, interglacials/interstadials can be distinguished by shrub-dominated regional vegetation (*Betula–Alnus–Salix*). Correspondingly, increases in CLDE biome affinity scores and simultaneous decreases in STEP biome scores characterize the interglacials/interstadials, and an opposite composition is shown by glacials/stadials. Over the Quaternary, a long-term decreasing trend in the tree and shrub population size was detected, which was accompanied by a reduction in floristic richness.
2. The cyclical pattern of the Arctic glacial–interglacial climate was primarily forced by the Earth's orbital parameters. High CLDE biome scores during interglacial periods are closely in phase with shifts of obliquity values from maxima to minima, thus highlighting the significance of obliquity driving Arctic vegetation successions during the Quaternary.
3. The regional climate and vegetation was further modulated by internal forcings of the Earth system. This is most pronounced for the first large glaciation during the MIS 24–22 interval, when global cooling may have prevented snow melt and led to an extended ice volume. This in turn probably caused strong snow- and ice-albedo feedback effects that aggravated glacial conditions and caused a significant decline in plant diversity and populations of trees and shrubs.
4. During the MPT, the ice volume effect exerted significant influences in both high and middle latitudes. In the low latitudes, the vegetation change showed strong imprints of SST changes, with an increasingly pronounced effect of glacial–interglacial cycles since the middle MPT.

Supporting information

Additional supporting information can be found in the online version of this article.

Figure S1. Comparison of the results of pollen taxon richness (*S*) and palynological richness $E(T_n)$ ($n = 100$, 200, 300, 400 and 500, respectively).

Acknowledgements. The drilling operation at Lake El'gygytgyn was financed by the International Continental Scientific Drilling Program (ICDP), the US National Science Foundation (NSF; grants OPP 007122, 96-15768 and 0002643), the German Federal Ministry of Education and Research (BMBF; grant 03G0642), Alfred Wegener Institute (AWI) and GeoForschungsZentrum Potsdam (GFZ), the Russian Academy of Sciences Far East Branch (RAS FEB), the Russian Foundation for Basic Research (RFBR), and the Austrian Federal Ministry of Science and Research (BMWF). The Russian GLAD 800 drilling system was developed and operated by DOSECC Inc. LacCore at the University of Minnesota handled core curation. We thank Prof. Yan Zhao for constructive advice on the manuscript. This study was supported by the National Natural Science Foundation of China (grants 42171157 and 41907379), the Education Department of Jiangsu Province (grants 18KJB170020 and 19KJB170026), the Jiangsu Shuangchuang Project (grants 06141008 and 06141009), and the PLOT projects of the German BMBF (grants 03G0859A and 03F0830A). The work of A. Andreev was also partly supported by the Russian Science Foundation (grant 20-17-00135). We thank the editor, Chronis Tzedakis, and other two anonymous reviewers for their constructive comments and suggestions.

Abbreviations. Bsi, biogenic silica; CLDE, cold deciduous forest; COCO, cool conifer forest; ICE, Incidence-based Coverage Estimator; MIS, Marine Isotope Stage; MPT, Mid-Pleistocene Transition; MS, magnetic susceptibility; NPP, non-pollen-palynomorph; SST, sea surface temperature; STEP, steppe; TAIG, taiga; TOC, total organic carbon; TUND, tundra.

References

Anderson PM, Brubaker LB. 1993. Holocene vegetation and climate histories of Alaska. In *Global Climates Since the Last Glacial*

Maximum, Wright, Jr. HE, Kutzbach JE, Webb, III T *et al.* (eds). University of Minnesota Press: Minneapolis; 386–400.

Anderson PM, Lozhkin AV, Belaya BV *et al.* 2002a. Modern spore–pollen spectra from the mountain regions of the Kolyma and Indigirka Rivers from lacustrine sediments. In *Quaternary Paleogeography of Beringia (in Russian)*, Simakov KV (ed.). NEISRI FEB RAS: Magadan; 28–39.

Anderson PM, Lozhkin AV, Belaya BV *et al.* 2002b. Modern spore–pollen spectra of northern Priokhot'ye from lacustrine sediments. In *Quaternary Paleogeography of Beringia (in Russian)*, Simakov KV (ed). NEISRI FEB RAS: Magadan; 51–61.

Andreev AA, Klimanov VA, Sulerzhitsky LD. 2001. Vegetation and climate history of the Yana River lowland, Russia, during the last 6400 yr. *Quaternary Science Reviews* **20**: 259–266. https://doi.org/10.1016/S0277-3791(00)00118-9

Andreev AA, Tarasov PE, Wennrich V *et al.* 2014. Late Pliocene and Early Pleistocene environments of the north-eastern Russian Arctic inferred from the Lake El'gygytgyn pollen record. *Climate of the Past* **9**: 4599–4653.

Andreev AA, Tarasov PE, Wennrich V *et al.* 2016. Millennial-scale vegetation changes in the north-eastern Russian Arctic during the Pliocene/Pleistocene transition (2.7–2.5 Ma) inferred from the pollen record of Lake El'gygytgyn. *Quaternary Science Reviews* **147**: 245–258. https://doi.org/10.1016/j.quascirev.2016.03.030

Belikovich AV. 1994. Recreation sources of planned "El'gygytgyn Lake Park" (in Russian). FEB RAS. *Vestnik* **3**: 57–63.

Berger A, Loutre MF. 2004. Astronomical theory of climate change. *Journal de Physique IV* **121**: 1–35. https://doi.org/10.1051/jp4:2004121001

Birks HJB, Felde VA, Bjune AE *et al.* 2016. Does pollen-assemblage richness reflect floristic richness? A review of recent developments and future challenges. *Review of Palaeobotany and Palynology* **228**: 1–25. https://doi.org/10.1016/j.revpalbo.2015.12.011

Birks HJB, Line JM. 1992. The use of rarefaction analysis for estimating palynological richness from Quaternary pollen-analytical data. *Holocene* **2**: 1–10. https://doi.org/10.1177/095968369200200101

Bobrov AE, Kupriyanova LA, Litvintseva MV *et al.* 1983. *Spores and Pollen of Gymnosperms from the Flora of the European Part of the USSR (in Russian)*. Nauka: Leningrad.

Brigham-Grette J, Melles M, Minyuk P *et al.* 2013. Pliocene warmth, extreme polar amplification, and stepped Pleistocene cooling recorded in NE Russia. *Science* **340**: 1421–1427. https://doi.org/10.1126/science.1233137

Calov R, Ganopolski A, Claussen M *et al.* 2005. Transient simulation of the last glacial inception. Part I: glacial inception as a bifurcation in the climate system. *Climate Dynamics* **24**: 545–561. https://doi.org/10.1007/s00382-005-0007-6

Chen C, Litt T. 2018. Dead Sea pollen provides new insights into the paleoenvironment of the southern Levant during MIS 6–5. *Quaternary Science Reviews* **188**: 15–27. https://doi.org/10.1016/j.quascirev.2018.03.029

Clark PU, Archer D, Pollard D *et al.* 2006. The Middle Pleistocene transition: characteristics, mechanisms, and implications for long-term changes in atmospheric pCO2. *Quaternary Science Reviews* **25**: 3150–3184. https://doi.org/10.1016/j.quascirev.2006.07.008

Cohen KM, Gibbard PL. 2019. Global chronostratigraphical correlation table for the last 2.7 million years, version 2019 QI-500. *Quaternary International* **500**: 20–31.

Colwell RK. 2013 EstimateS: Statistical Estimation of Species Richness and Shared Species from Samples. version 9. User's Guide and application published at: purl.oclc.org/estimates.

Cronin TM, Kitamura A, Ikeya N *et al.* 1994. Late Pliocene climate change 3.4–2.3 Ma: paleoceanographic record from the Yabuta Formation, Sea of Japan. *Palaeogeography, Palaeoclimatology, Palaeoecology* **108**: 437–455. https://doi.org/10.1016/0031-0182(94)90245-3

Ding ZL, Derbyshire E, Yang SL *et al.* 2002. Stacked 2.6-Ma grain size record from the Chinese loess based on five sections and correlation with the deep-sea δ18O record. *Paleoceanography and Paleoclimatology* **17**: 5–1-5-21.

Fægri K, Iversen J. 1989. *Textbook of Pollen Analysis*. 4th edn. John Wiley & Sons: London.

Fang XM, Yan MD, Van der Voo R *et al.* 2005. Late Cenozoic deformation and uplift of the NE Tibetan Plateau: evidence from high-resolution magneto stratigraphy of the Guide Basin, Qinghai Province, China. *Geological Society of America Bulletin* **117**: 1208–1225. https://doi.org/10.1130/B25727.1

Fang XM, Zhang WL, Meng QQ *et al.* 2007. High-resolution magnetostratigraphy of the Neogene Huaitoutala section in the eastern Qaidam Basin on the NE Tibetan Plateau, Qinghai Province, China and its implication on tectonic uplift of the NE Tibetan Plateau. *Earth and Planetary Science Letters* **258**: 293–306. https://doi.org/10.1016/j.epsl.2007.03.042

Fedorov G, Nolan M, Brigham-Grette J *et al.* 2013. Preliminary estimation of Lake El'gygytgyn water balance and sediment income. *Climate of the Past* **9**: 1455–1465. https://doi.org/10.5194/cp-9-1455-2013

Felde VA, Peglar SM, Bjune AE *et al.* 2016. Modern pollen-plant richness and diversity relationships exist along a vegetational gradient in southern Norway. *Holocene* **26**: 163–175. https://doi.org/10.1177/0959683615596843

Fischer H, Wahlen M, Smith J *et al.* 1999. Ice core records of atmospheric CO2 around the last three glacial terminations. *Science* **283**: 1712–1714. https://doi.org/10.1126/science.283.5408.1712

Forman SL, Pierson J, Gómez J *et al.* 2006. Luminescence geochronology for sediments from Lake El'gygytgyn, northeast Siberia, Russia: constraining the timing of paleoenvironmental events for the past 200 ka. *Journal of Paleolimnology* **37**: 77–88. https://doi.org/10.1007/s10933-006-9024-7

Francke A, Wennrich V, Sauerbrey M *et al.* 2013. Multivariate statistic and time series analyses of grain-size data in quaternary sediments of Lake El'gygytgyn, NE Russia. *Climate of the Past* **9**: 2459–2470. https://doi.org/10.5194/cp-9-2459-2013

Gaston KJ. 1996. Species richness: measure and measurement. In *Biodiversity. A Biology of Numbers and Differences*, Gaston KJ (ed). Blackwell Science Ltd: Oxford; 77–113.

Haltia EM, Nowaczyk NR. 2014. Magnetostratigraphy of sediments from Lake El'gygytgyn ICDP Site 5011-1: paleomagnetic age constraints for the longest paleoclimate record from the continental Arctic. *Climate of the Past* **10**: 623–642. https://doi.org/10.5194/cp-10-623-2014

Hammer Ø, Harper DAT, Ryan PD. 2001. PAST: paleontological statistics software package for education and data analysis. *Palaeontogr Electro* **4**: 9.

Harper DAT. (1999) *Numerical Palaeobiology*. New York: John Wiley & Sons.

Hays JD, Imbrie J, Shackleton NJ. 1976. Variations in the Earth's orbit: pacemaker of the ice ages. *Science* **194**: 1121–1132. https://doi.org/10.1126/science.194.4270.1121

Herzschuh U, Birks HJB, Laepple T *et al.* 2016. Glacial legacies on interglacial vegetation at the Pliocene–Pleistocene transition in NE Asia. *Nature Communications* **7**: 11967. https://doi.org/10.1038/ncomms11967

Juschus O, Melles M, Gebhardt AC *et al.* 2009. Late Quaternary mass movement events in Lake Elâ'gygytgyn, North-eastern Siberia. *Sedimentology* **56**: 2155–2174. https://doi.org/10.1111/j.1365-3091.2009.01074.x

Kalnay EM, Kanamitsu M, Kistler R *et al.* 1996. The NCEP/NCAR 40-year reanalysis project. *Bulletin of the American Meteorological Society* **77**: 437–471. https://doi.org/10.1175/1520-0477(1996)077<0437:TNYRP>2.0.CO;2

Kataoka H, Takahara H, Krivonogov SK *et al.* 2003. Pollen record from the Chivyrkui Bay outcrop on the eastern shore of Lake Baikal since the Late Glacial, long continental record from Lake Baikal. In *Long Continental Records from Lake Baikal*, Kashiwaya K (ed). Springer: Tokyo; 207–218.

Kitamura A, Kawagoe T. 2006. Eustatic sea-level change at the Mid-Pleistocene climate transition: new evidence from the shallow-marine sediment record of Japan. *Quaternary Science Reviews* **25**: 323–335. https://doi.org/10.1016/j.quascirev.2005.02.009

Kupriyanova LA, Alyoshina LA 1972. Pollen and Spores of Plants from the Flora of European Part of USSR Vol. I. (in Russian). Academy of Sciences USSR, Komarov Botanical Institute: Leningrad.

Laskar J, Robutel P, Joutel F *et al.* 2004. A long-term numerical solution for the insolation quantities of the Earth. *Astronomy and Astrophysics* **428**: 261–285. https://doi.org/10.1051/0004-6361:20041335

Layer PW. 2000. Argon-40/argon-39 age of the El'gygytgyn impact event, Chukotka, Russia. *Meteoritics and Planetary Science* **35**: 591–599. https://doi.org/10.1111/j.1945-5100.2000.tb01439.x

Li JJ. 1995. Uplift of Qinghai-Xizang (Tibet) Plateau and Global Change (in Chinese). Lanzhou University Press: Lanzhou.

Li Q. 2018. Spatial variability and long-term change in pollen diversity in Nam Co catchment (central Tibetan Plateau): implications for alpine vegetation restoration from a paleoecological perspective. *Science China Earth Sciences* **61**: 270–284. https://doi.org/10.1007/s11430-017-9133-0

Lisiecki LE, Raymo ME. 2005. A Pliocene–Pleistocene stack of 57 globally distributed benthic δ18O records. *Paleoceanography* **20**: PA1003.

Liu JB, Shen ZW, Chen W *et al.* 2021. Dipolar mode of precipitation changes between north China and the Yangtze River Valley existed over the entire Holocene: evidence from the sediment record of Nanyi Lake. *International Journal of Climatology* **41**: 1667–1681. https://doi.org/10.1002/joc.6906

Liu XK, Liu JB, Chen SQ *et al.* 2020. New insights on Chinese cave δ18O records and their paleoclimatic significance. *Earth-Science Reviews* **207**. https://doi.org/10.1016/j.earscirev.2020.103216 [PubMed: 103216]

Lozhkin AV, Anderson PM. 2013. Vegetation responses to interglacial warming in the Arctic: examples from Lake El'gygytgyn, Far East Russian Arctic. *Climate of the Past* **9**: 1211–1219. https://doi.org/10.5194/cp-9-1211-2013

Lozhkin AV, Anderson PM, Belaya BV *et al.* 2002. Reflections on modern pollen rain of Chukotka from bottom lake sediments (in Russian). In *Quaternary Paleogeography of Beringia*, Neisri FEB, Simakov KV (ed). Russian Academy of Sciences: Magadan; 40–50.

Lozhkin AV, Anderson PM, Matrosova TV *et al.* 2006. The pollen record from El'gygytgyn Lake: implications for vegetation and climate histories of northern Chukotka since the late Middle Pleistocene. *Journal of Paleolimnology* **37**: 135–153. https://doi.org/10.1007/s10933-006-9018-5

Lozhkin AV, Anderson PM, Vartanyan SL *et al.* 2001. Late Quaternary paleoenvironments and modern pollen data from Wrangel Island (Northern Chukotka). *Quaternary Science Reviews* **20**: 217–233. https://doi.org/10.1016/S0277-3791(00)00121-9

Lozhkin AV, Minyuk PS, Anderson PM *et al.* 2017. Variability in landscape and lake system responses to glacial and interglacial climates during the Middle Pleistocene based on palynological and geochemical data from Lake El'gygytgyn, eastern Arctic. *Review of Palaeobotany and Palynology* **246**: 1–13. https://doi.org/10.1016/j.revpalbo.2017.06.004

Maharaj D, Elbra T, Pesonen LJ. 2013. Physical properties of the drill core from the El'gygytgyn impact structure. *NE Russia. Meteoritics and Planetary Science* **48**: 1130–1142. https://doi.org/10.1111/maps.12064

Maslin MA, Brierley CM. 2015. The role of orbital forcing in the Early Middle Pleistocene Transition. *Quaternary International* **389**: 47–55. https://doi.org/10.1016/j.quaint.2015.01.047

Maslin MA, Ridgwell AJ. 2005. Mid-Pleistocene revolution and the 'eccentricity myth'. In Early–Middle Pleistocene Transitions: the Land-Ocean Evidence, Head MJ, Gibbard PL (eds). Special Publication Geological Society of London 247: 19–34.

Matrosova TV. 2009. Klimat i rastitel'nost' Anadyrskogo ploskogor'ya za poslednie 350 tys. let (palinologicheskaya kharakteristika osadkov oz. El'gygytgyn) (Climate and vegetation of Anadyr Plateau during the last 350 ka (palynological characteristic of Lake El'gygytgyn sediments) (in Russian). PhD Thesis, Magadan.

Matthias I, Semmler MSS, Giesecke T. 2015. Pollen diversity captures landscape structure and diversity. *Journal of Ecology* **103**: 880–890. https://doi.org/10.1111/1365-2745.12404

Melles M, Brigham-Grette J, Glushkova OY *et al.* 2006. Sedimentary geochemistry of core PG1351 from Lake El'gygytgyn – a sensitive record of climate variability in the East Siberian Arctic during the past three glacial–interglacial cycles. *Journal of Paleolimnology* **37**: 89–104. https://doi.org/10.1007/s10933-006-9025-6

Melles M, Brigham-Grette J, Minyuk P *et al.* 2011. The Lake El'gygytgyn Scientific Drilling Project – Conquering Arctic Challenges through Continental Drilling. *Scientific Drilling* **11**: 29–40. https://doi.org/10.5194/sd-11-29-2011

Melles M, Brigham-Grette J, Minyuk PS *et al.* 2012. 2.8 million years of arctic climate change from lake El'gygytgyn, NE Russia. *Science* **337**: 315–320. https://doi.org/10.1126/science.1222135

Milankovitch M. 1941. Kanon der Erdbestrahlung und seine Anwendung auf das Eiszeitenproblem. In Posebna izdanja Srpske kraljevske akademije (Special editions of Serbian Royal Academy) CXXIII.

Müller S, Tarasov PE, Andreev AA *et al.* 2010. Late Quaternary vegetation and environments in theVerkhoyansk Mountains region (NE Asia) reconstructed from a 50-kyr fossil pollen record from Lake Billyakh. *Quaternary Science Reviews* **29**: 2071–2086. https://doi.org/10.1016/j.quascirev.2010.04.024

Naish T, Kamp PJJ, Pillans B. 1997. Recurring global sea-level changes recorded in shelf deposits near the G/M polarity transition, Wanganui Basin, New Zealand: implications for redefining the Pliocene–Pleistocene boundary. *Quaternary International* **40**: 61–71. https://doi.org/10.1016/S1040-6182(96)00062-6

Naish TR, Abbott ST, Alloway V *et al.* 1998. Astronomical calibration of a Southern Hemisphere Plio-Pleistocene reference section, Wanganui Basin, New Zealand. *Quaternary Science Reviews* **17**: 695–710. https://doi.org/10.1016/S0277-3791(97)00075-9

Nolan M. 2013. Quantitative and qualitative constraints on hind-casting the formation of multiyear lake-ice covers at Lake El'gygytgyn. *Climate of the Past* **9**: 1253–1269. https://doi.org/10.5194/cp-9-1253-2013

Nolan M, Brigham-Grette J. 2006. Basic hydrology, limnology, and meteorology of modern Lake El'gygytgyn, Siberia. *Journal of Paleolimnology* **37**: 17–35. https://doi.org/10.1007/s10933-006-9020-y

Nolan M, Liston G, Prokein P *et al.* 2002. Analysis of lake ice dynamics and morphology on Lake El'gygytgyn, NE Siberia, using synthetic aperture radar (SAR) and Landsat. *Journal of Geophysical Research* **108**: 8162–8174. https://doi.org/10.1029/2001JD000934

Nowaczyk NR, Haltia EM, Ulbricht D *et al.* 2013. Chronology of Lake El'gygytgyn sediments – a combined magnetostratigraphic, palaeoclimatic and orbital tuning study based on multi-parameter analyses. *Climate of the Past* **9**: 2413–2432. https://doi.org/10.5194/cp-9-2413-2013

Prentice C, Guiot J, Huntley B *et al.* 1996. Reconstructing biomes from palaeoecological data: a general method and its application to European pollen data at 0 and 6 ka. *Climate Dynamics* **12**: 185–194. https://doi.org/10.1007/BF00211617

Prentice IC, Webb III, T. 1998. BIOME 6000: reconstructing global mid-Holocene vegetation patterns from palaeoecological records. *Journal of Biogeography* **25**: 997–1005. https://doi.org/10.1046/j.1365-2699.1998.00235.x

Prokopenko AA, Hinnov LA, Williams DF *et al.* 2006. Orbital forcing of continental climate during the Pleistocene: a complete astronomically tuned climatic record from Lake Baikal, SE Siberia. *Quaternary Science Reviews* **25**: 3431–3457. https://doi.org/10.1016/j.quascirev.2006.10.002

Reille M. 1992. Pollen et spores d'Europe et d'Afrique du nord. Laboratoire de Botanique Historique et Palynologie: Marseille.

Reille M. 1995. Pollen et spores d'Europe et d'Afrique du nord, Suppl. 1. Laboratoire de Botanique Historique et Palynologie: Marseille.

Reille M. 1998. Pollen et spores d'Europe et d'Afrique du nord, Suppl. 2. Laboratoire de Botanique Historique et Palynologie: Marseille.

Rudaya N, Tarasov PE, Dorofeyuk N *et al.* 2009. Holocene environments and climate in the Mongolian Altai reconstructed from the Hoton-Nur pollen and diatom records: a step towards better understanding climate dynamics in Central Asia. *Quaternary Science Reviews* **28**: 540–554. https://doi.org/10.1016/j.quascirev.2008.10.013

Ruddiman WF, Kutzbach JE. 1989. Forcing of late Cenozoic northern hemisphere climate by plateau uplift in southern Asia and the American west. *Journal of Geophysical Research* **94**: 18409–18427. https://doi.org/10.1029/JD094iD15p18409

Sauerbrey MA, Juschus O, Gebhardt AC *et al.* 2013. Mass movement deposits in the 3.6-Ma sediment record of Lake El'gygytgyn, Far East Russian Arctic. *Climate of the Past* **9**: 1949–1967. https://doi.org/10.5194/cp-9-1949-2013

Schefuß E, Schouten S, Jansen JHF *et al.* 2003. African vegetation controlled by tropical sea surface temperatures in the mid-Pleistocene period. *Nature* **422**: 418–421. https://doi.org/10.1038/nature01500

Schefuβ E, Sinninghe Damste JSS, Jansen JHF. 2004. Forcing of tropical Atlantic sea surface temperatures during the mid-Pleistocene transition. *Paleoceanography* **19**: PA4029.

Schmieder F, von Dobeneck T, Bleil U. 2000. The Mid-Pleistocene climate transition as documented in the deep South Atlantic Ocean: initiation, interim state and terminal event. *Earth and Planetary Science Letters* **179**: 539–549. https://doi.org/10.1016/S0012-821X(00)00143-6

Shackleton NJ, Berger A, Peltier WR. 1990. An alternative astronomical calibration of the Lower Pleistocene timescale based on ODP Site 677. *Transactions of the Royal Society of Edinburgh: Earth Sciences* **81**: 251–261. https://doi.org/10.1017/S0263593300020782

Shackleton NJ, Opdyke ND. 1973. Oxygen isotope and palaeomagnetic stratigraphy of Equatorial Pacific core V28-238: oxygen isotope temperatures and ice volumes on a 105 year and 106 year scale. *Quaternary Research* **3**: 39–55. https://doi.org/10.1016/0033-5894(73)90052-5

Shackleton NJ, Opdyke ND. 1976. Oxygen-isotope and paleomagnetic stratigraphy of pacific core V28-239 Late Pliocene to latest Pleistocene. In *Investigations of Late Quaternary Paleoceanography and Paleoclimatology*, Cline R, Hays J (eds). Geological Society of America, 449–464.

Shahgedanova M, Perov V, Mudrov Y. 2002. The mountains of northern Russia. In *The Physical Geography of Northern Eurasia*, Shahgedanova M (ed). Oxford University Press: Oxford; 284–313.

Shannon CE. 1948. A mathematical theory of communication. *Bell System Technical Journal* **27**: 379–423. https://doi.org/10.1002/j.1538-7305.1948.tb01338.x

Siegenthaler U, Stocker TF, Monnin E *et al*. 2005. Stable carbon cycle climate relationship during the Late Pleistocene. *Science* **310**: 1313–1317. https://doi.org/10.1126/science.1120130

Stockmarr J. 1971. Tablets with spores used in absolute pollen analysis. *Pollen et Spores* **13**: 615–621.

Sun Y, Yin Q, Crucifix M *et al*. 2019. Diverse manifestations of the mid-Pleistocene climate transition. Nature. *Communications* **10**: 1–11.

Swann GEA, Leng MJ, Juschus O *et al*. 2010. A combined oxygen and silicon diatom isotope record of Late Quaternary change in Lake El'gygytgyn, North East Siberia. *Quaternary Science Reviews* **29**: 774–786. https://doi.org/10.1016/j.quascirev.2009.11.024

Tarasov PE, Andreev AA, Anderson PM *et al*. 2013. A pollen-based biome reconstruction over the last 3.562 million years in the Far East Russian Arctic – new insights into climate–vegetation relationships at the regional scale. *Climate of the Past* **9**: 2759–2775. https://doi.org/10.5194/cp-9-2759-2013

Torres V, Hooghiemstra H, Lourens L *et al*. 2013. Astronomical tuning of long pollen records reveals the dynamic history of montane biomes and lake levels in the tropical high Andes during the Quaternary. *Quaternary Science Reviews* **63**: 59–72. https://doi.org/10.1016/j.quascirev.2012.11.004

Tzedakis PC, Crucifix M, Mitsui T *et al*. 2017. A simple rule to determine which insolation cycles lead to interglacials. *Nature* **542**: 427–432. https://doi.org/10.1038/nature21364

Tzedakis PC, Hooghiemstra H, Pälike H. 2006. The last 1.35 million years at Tenaghi Philippon: revised chronostratigraphy and long-term vegetation trends. *Quaternary Science Reviews* **25**: 3416–3430. https://doi.org/10.1016/j.quascirev.2006.09.002

Tzedakis PC, McManus JF, Hooghiemstra H *et al*. 2003. Comparison of changes in vegetation in northeast Greece with records of climate variability on orbital and suborbital frequencies over the last 450000 years. *Earth and Planetary Science Letters* **212**: 197–212. https://doi.org/10.1016/S0012-821X(03)00233-4

van Geel B. 2001. Non-pollen palynomorphs. In *Tracking Environmental Changes Using Lake Sediments, Vol. 3: Terrestrial, algal and silicaceous indicators*, Smol JP, Birks HJB, Last WM *et al*. (eds). Kluwer Publishers: Dordrecht; 99–119.

Wagner B, Vogel H, Francke A *et al*. 2019. Mediterranean winter rainfall in phase with African monsoons during the past 1.36 million years. *Nature* **573**: 256–260. https://doi.org/10.1038/s41586-019-1529-0

Wennrich V, Andreev AA, Tarasov PE *et al*. 2016. Impact processes, permafrost dynamics, and climate and environmental variability in the terrestrial Arctic as inferred from the unique 3.6 Myr record of Lake El'gygytgyn, Far East Russia – a review. *Quaternary Science Reviews* **147**: 221–244. https://doi.org/10.1016/j.quascirev.2016.03.019

Wennrich V, Francke A, Dehnert A *et al*. 2013. Modern sedimentation patterns in Lake El'gygytgyn, NE Russia, derived from surface sediment and inlet streams samples. *Climate of the Past* **9**: 135–148. https://doi.org/10.5194/cp-9-135-2013

Wennrich V, Minyuk PS, Borkhodoev V *et al*. 2014. Pliocene to Pleistocene climate and environmental history of Lake El'gygytgyn, Far East Russian Arctic, based on high-resolution inorganic geochemistry data. *Climate of the Past* **10**: 1381–1399. https://doi.org/10.5194/cp-10-1381-2014

Whitney BS, Mayle FE, Burn MJ *et al*. 2014. Sensitivity of Bolivian seasonally dry tropical forest to precipitation and temperature changes over glacial–interglacial timescales. *Vegetation History and Archaeobotany* **23**: 1–14. https://doi.org/10.1007/s00334-013-0395-1

Williams JW, Shuman BN, Webb III, T *et al*. 2004. Late Quaternary vegetation dynamics in North America: scaling from taxa to biomes. *Ecological Monographs* **74**: 309–334. https://doi.org/10.1890/02-4045

Willis KJ, Kleczkowski A, New M *et al*. 2007. Testing the impact of climate variability on European plant diversity: 320 000 years of water–energy dynamics and its long-term influence on plant taxonomic richness. *Ecology Letters* **10**: 673–679. https://doi.org/10.1111/j.1461-0248.2007.01056.x

Xiao XY, Shen J, Wang SM *et al*. 2008. The plant diversity and its relationship with paleoenvironment since 2.78 Ma revealed by pollen records in the Heqing deep drilling core. *Chinese Science Bulletin* **53**: 3686–3698. https://doi.org/10.1007/s11434-008-0439-6

Zander A, Hilgers A. 2013. Potential and limits of OSL, TT-OSL, IRSL and pIRIR290 dating methods applied on a Middle Pleistocene sediment record of Lake El'gygytgyn, Russia. *Climate of the Past* **9**: 719–733. https://doi.org/10.5194/cp-9-719-2013

Zhao W, Andreev AA, Tarasov PE *et al*. 2019. Vegetation and climate during the penultimate interglacial of the northeastern Russian Arctic: the Lake El'gygytgyn pollen record. *Boreas* **48**: 507–515. https://doi.org/10.1111/bor.12373

Zhao WW, Andreev AA, Wennrich V *et al*. 2015. The Réunion Subchron vegetation and climate history of the northeastern Russian Arctic inferred from the Lake El'gygytgyn pollen record. *Palaeogeography, Palaeoclimatology, Palaeoecology* **436**: 167–177. https://doi.org/10.1016/j.palaeo.2015.06.047

Zhao WW, Tarasov PE, Lozhkin AV *et al*. 2018. High-latitude vegetation and climate changes during the Mid-Pleistocene Transition inferred from a palynological record from Lake El'gygytgyn, NE Russian Arctic. *Boreas* **47**: 137–149. https://doi.org/10.1111/bor.12262

Zhao Y, Tzedakis PC, Li Q *et al*. 2020. Evolution of vegetation and climate variability on the Tibetan Plateau over the past 1.74 million years. Science Advances 6: eaay 6193. https://doi.org/10.1126/sciadv.aay6193

